ACUSTICA · acta acustica
Vol. 84 (1998) 495 – 502



# Anisotropic Attenuation and Material Symmetry

J. M. Carcione, F. Cavallini
Osservatorio Geofisico Sperimentale di Trieste, P. O. Box 2011, I-34016 Trieste, Italy

Klaus Helbig
Kiebitzrain 84, D-30657 Hannover, Germany

**Summary**
The internal structure of a material (as, e.g., expressed by the stiffnesses) dictates the dependence of the quality factor $Q$ on direction. Therefore, the attenuation should have *at least* the symmetry of the crystallographic form of the material. To investigate this property, we compare three different constitutive equations for modeling anisotropic attenuation of wave propagation in rocks. The present analysis considers media with symmetries ranging from orthorhombic to transversely isotropic with the anelasticity described by a relaxation model.
The first stress-strain relation is based on Backus's averaging theory, which provides the best model for laminated media. The other two constitutive laws are not restricted to stratified media and can be tested with the first model. The second constitutive law is based on the following mechanical interpretation: Each eigenvector (called eigenstrain) of the stiffness tensor of an anisotropic solid defines a fundamental deformation state of the medium. The six eigenvalues (called eigenstiffnesses) represent the genuine elastic parameters, which generalize to relaxation functions in the anelastic case. The third constitutive equation satisfies the condition that the mean stress depends only on the dilatational relaxation function in any coordinate system (the trace of the stress tensor is invariant under coordinate transformations). Moreover, the deviatoric stresses solely depend on the shear relaxation function.
The last two constitutive relations yield similar results when modeling a laminated medium, but they differ for an orthorhombic medium. Tests on available experimental data indicate that the second model provides the best fitting.

PACS no. 43.20.Jr, 43.35.Cg, 43.35.Fj

## Introduction

The so-called Neumann's principle [1, 2] states, roughly speaking, that the symmetry of the consequences is at least as high as that of the causes. This implies that any kind of symmetry possessed by wave attenuation must be present within the crystallographic class of the material. Actually Pierre Curie, who was a true scientific leader in crystallography, already in 1884 clearly stated this symmetry principle in an article on the *Bull. Soc. Mineral. France*.

Since attenuation can be explained by a large number of mechanisms, it is difficult, if not impossible, to build a general microstructural theory. A phenomenological theory, such as viscoelasticity, leads to a convenient model. Though such a model does not allow to predict attenuation levels, it can be used to estimate the anisotropic attenuation. The problem is the determination of the time (or frequency) dependence of the relaxation tensor (21 components in triclinic media; e.g., see [3]). Most applications use the Kelvin-Voigt constitutive law, based on 21 independent viscosity functions [4], corresponding to imaginary constants in the frequency domain. Sometimes it has been possible to estimate all these constants satisfactorily [5]. However, in the present article three alternative models are shown based on fewer parameters, which are not the imaginary elasticities in themselves, but real quality factors (often more readily available in the seismic practice).

Received 18 November 1996,
accepted 17 July 1997.

Attenuation is a characteristic associated to a deformation state of the medium (e.g., a wave mode) and therefore a small number of parameters should suffice to obtain the relaxation components. In isotropic media, two (dilatational and shear) relaxation functions completely define the anelastic properties. For finely layered media, Backus's averaging is a physically sound approach for obtaining the relaxation components of a transversely isotropic (TI) medium [6]. Two alternative constitutive laws [7, 8], not restricted to layered media as Backus's approach, relate waves and deformation modes to anelastic processes, using at most six relaxation functions.

Dissipation in a given direction is quantified by the quality factor or the related attenuation factor, which can be measured experimentally by various techniques (e.g., [9]). Most experimental data about anisotropic attenuation were obtained in the laboratory at ultrasonic frequencies, whereas such data are not ususally collected during seismic surveys. This lack of data constitutes a serious problem because, unlike the slownesses, the attenuation behaviour observed at those frequency ranges cannot be extrapolated to the sonic and seismic ranges, since the mechanisms of dissipation can be quite different in different frequency ranges.

Hosten *et al.* [5] measured the dependence of attenuation with propagation direction in a carbon-epoxy composite. They found that, in a sense, attenuation is more anisotropic than slowness, and while shear wave dissipation is larger than longitudinal dissipation in the isotropy planes, the opposite behaviour occurs in planes containing the axis of rotational symmetry. Arts *et al.* [10] obtained the viscoelastic tensor of

ACUSTICA · acta acustica
Vol. 84 (1998)

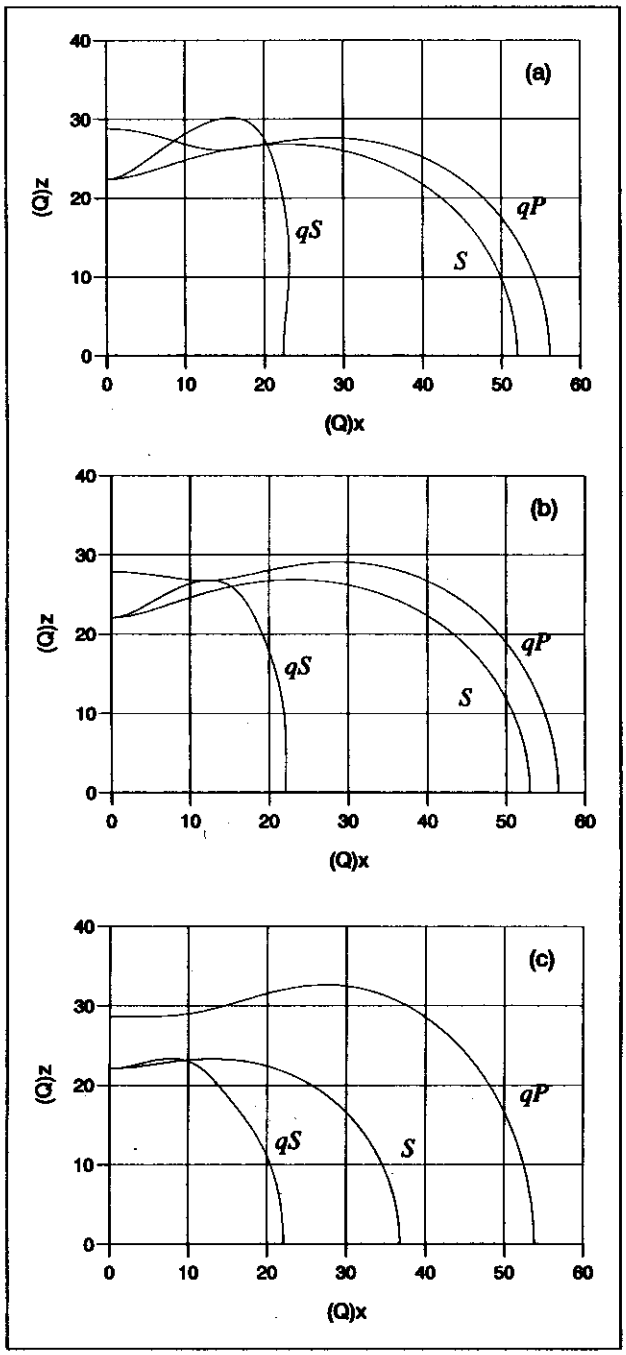


Figure 1. Polar representation of the quality factors for a hydrocarbon source rock, corresponding to model 1 (a), model 2 (b) and model 3 (c). The parameters of models 2 and 3 have been chosen so that their results be close to those of model 1, taken as giving synthetic data on which to test the flexibility of models 2 and 3.

dry and saturated rock samples (sandstone and limestone). Their results indicate that attenuation in dry rocks is one order of magnitude lower than attenuation in saturated samples. Moreover, the attenuation is again more anisotropic than the slowness, a fact that is interpreted by the authors as attenuation having lower symmetry than the slowness, or, alternatively, a consequence of experimental error. According to Baste *et al.* [11], the elastic stiffnesses are quite adequate to describe the closing of cracks – provided that the proper experimental techniques are employed. On the other hand, laboratory data obtained by Yin [12] on prestressed rocks suggest that attenuation may be more sensitive to the closing of cracks than the elastic stiffnesses, and that its symmetry is closely related to the type of loading. Yin found a simple relation between wave amplitude and loading stress, and concluded that accurate estimates of wave attenuation can be used to quantify stress-induced anisotropy.

## 1. Constitutive equations

The following rheological model assumes a single standard linear solid element [13] describing each anelastic deformation mode (identified by the index $\nu$), whose (dimensionless) complex moduli can be expressed as

$$M_\nu(\omega) = \frac{\sqrt{Q_{0\nu}^2+1}-1+\mathrm{i}\omega Q_{0\nu}\tau_0}{\sqrt{Q_{0\nu}^2+1}+1+\mathrm{i}\omega Q_{0\nu}\tau_0}, \qquad (1)$$

where $\omega$ is the angular frequency. Depending on the symmetry class, subscript $\nu$ goes from 1 to 6 at most; in the rheological models that follow $\nu = 1, 2$ in cases 1 and 3, and $\nu = 1, \ldots, 4$ in case 2. The quality factor $Q_\nu$, associated with each modulus, is equal to the real part of $M_\nu$ divided by its imaginary part. At $\omega_0 = 1/\tau_0$, the curve $Q_\nu(\omega)$ has its highest value: $Q_\nu(\omega_0) = Q_{0\nu}$. For a given angular frequency $\omega$, we take $\tau_0\omega = 1$; and, therefore, the frequency dependence is irrelevant. Actually, we are interested in the anisotropic properties of attenuation. The high-frequency limit corresponds to the elastic case with $M_\nu \to 1$.

Let us denote by $p_{IJ}$, where $I, J = 1, \ldots, 6$, the complex stiffnesses and by $c_{IJ}$ the purely elastic (or unrelaxed) stiffness constants. Then, $p_{IJ}(\omega \to \infty) = c_{IJ}$. For an orthorhombic medium, Hooke's Law can be written either in the so-called "Voigt notation" as

$$\begin{pmatrix} \sigma_{11} \\ \sigma_{22} \\ \sigma_{33} \\ \sigma_{23} \\ \sigma_{13} \\ \sigma_{12} \end{pmatrix} = \begin{pmatrix} p_{11} & p_{12} & p_{13} & 0 & 0 & 0 \\ p_{12} & p_{22} & p_{23} & 0 & 0 & 0 \\ p_{13} & p_{23} & p_{33} & 0 & 0 & 0 \\ 0 & 0 & 0 & p_{44} & 0 & 0 \\ 0 & 0 & 0 & 0 & p_{55} & 0 \\ 0 & 0 & 0 & 0 & 0 & p_{66} \end{pmatrix} \begin{pmatrix} \epsilon_{11} \\ \epsilon_{22} \\ \epsilon_{33} \\ 2\epsilon_{23} \\ 2\epsilon_{13} \\ 2\epsilon_{12} \end{pmatrix} \qquad (2)$$

or in "Kelvin notation" (required by model 2) as

$$\begin{pmatrix} \sigma_{11} \\ \sigma_{22} \\ \sigma_{33} \\ \sqrt{2}\sigma_{23} \\ \sqrt{2}\sigma_{13} \\ \sqrt{2}\sigma_{12} \end{pmatrix} = \qquad (3)$$

$$\begin{pmatrix} p_{11} & p_{12} & p_{13} & 0 & 0 & 0 \\ p_{12} & p_{22} & p_{23} & 0 & 0 & 0 \\ p_{13} & p_{23} & p_{33} & 0 & 0 & 0 \\ 0 & 0 & 0 & 2p_{44} & 0 & 0 \\ 0 & 0 & 0 & 0 & 2p_{55} & 0 \\ 0 & 0 & 0 & 0 & 0 & 2p_{66} \end{pmatrix} \begin{pmatrix} \epsilon_{11} \\ \epsilon_{22} \\ \epsilon_{33} \\ \sqrt{2}\epsilon_{23} \\ \sqrt{2}\epsilon_{13} \\ \sqrt{2}\epsilon_{12} \end{pmatrix},$$

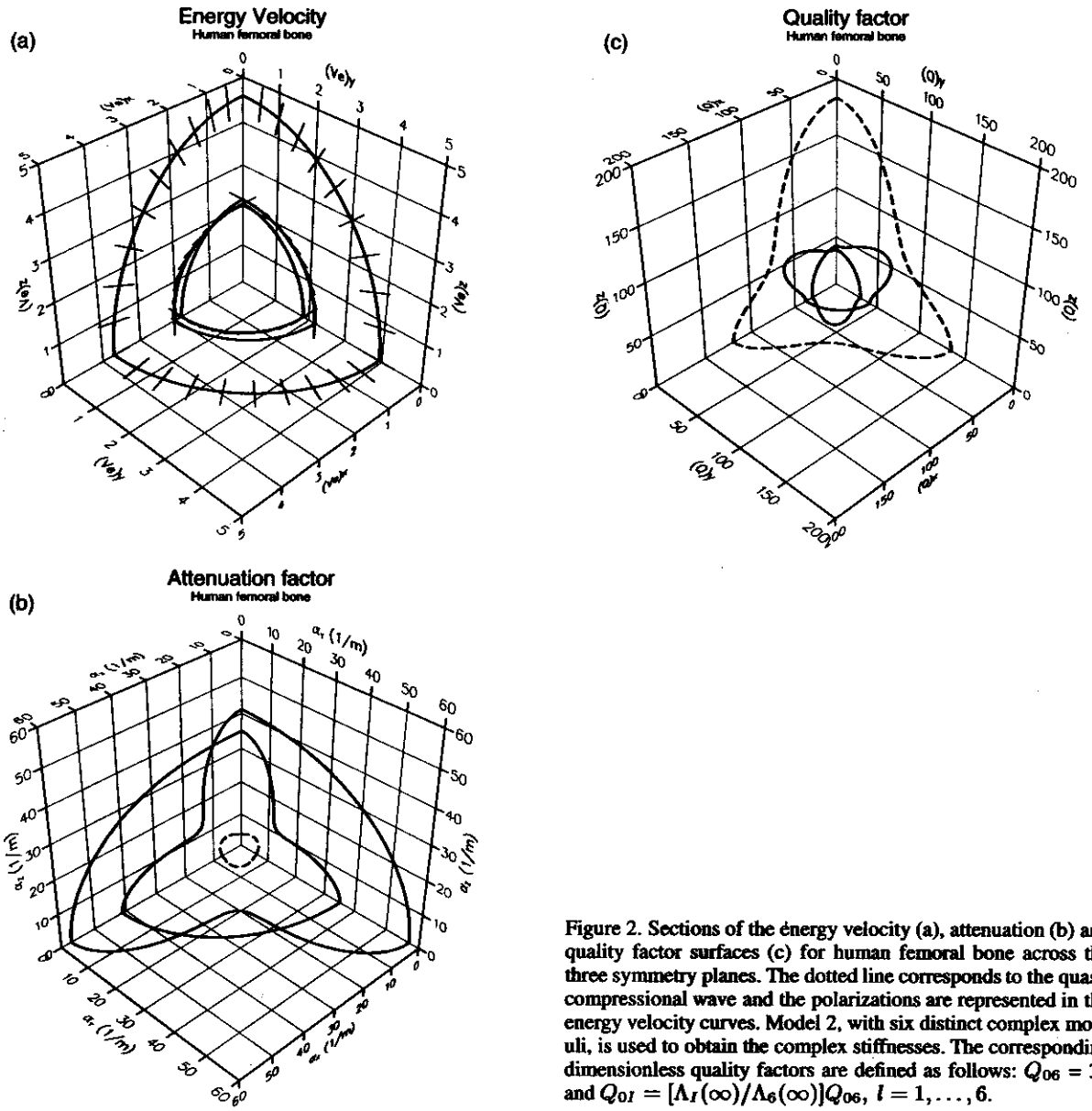


Figure 2. Sections of the energy velocity (a), attenuation (b) and quality factor surfaces (c) for human femoral bone across the three symmetry planes. The dotted line corresponds to the quasi-compressional wave and the polarizations are represented in the energy velocity curves. Model 2, with six distinct complex moduli, is used to obtain the complex stiffnesses. The corresponding dimensionless quality factors are defined as follows: $Q_{06} = 30$ and $Q_{0l} = [\Lambda_l(\infty)/\Lambda_6(\infty)]Q_{06}$, $l = 1, \ldots, 6$.

where the $p_{IJ}$ are functions of $c_{IJ}$ and $M_\nu$ [14]. Note that the three arrays of (3) are true tensors in 6-D space, while in equation (2) they are just arrays.

Transverse isotropy implies

$$p_{22} = p_{11}, \quad p_{23} = p_{13},$$
$$p_{44} = p_{55}, \quad p_{66} = (p_{11} - p_{12})/2. \tag{4}$$

### 1.1. Model 1: Effective anisotropy

Interlayering of lithologies with different material properties on a scale much finer than the dominant wavelength of the signal yields effective anisotropy [15]. Carcione [6] used this approach to study the anisotropic characteristics of attenuation in viscoelastic finely layered media. Let each medium be isotropic and anelastic with complex Lamé parameters given by

$$\lambda = \rho\left(V_P^2 - \frac{4}{3}V_S^2\right)M_1 - \frac{2}{3}\rho V_S^2 M_2$$
$$\text{and } \mu = \rho V_S^2 M_2, \tag{5}$$

where $M_1$ and $M_2$ are the dilatational and shear complex moduli, respectively, $V_P$ and $V_S$ are the elastic high-frequency limit compressional and shear velocities, and $\rho$ is the density (note that in [6] the elastic limit corresponds to the relaxed moduli). For instance [15],

$$p_{55} = \langle \mu^{-1} \rangle^{-1}, \quad \text{and} \quad p_{66} = \langle \mu \rangle, \tag{6}$$

where $\langle \bullet \rangle$ denotes the thickness weighted average. The complete equations can be found in [15]. In the case of a periodic

ACUSTICA · acta acustica
Vol. 84 (1998)

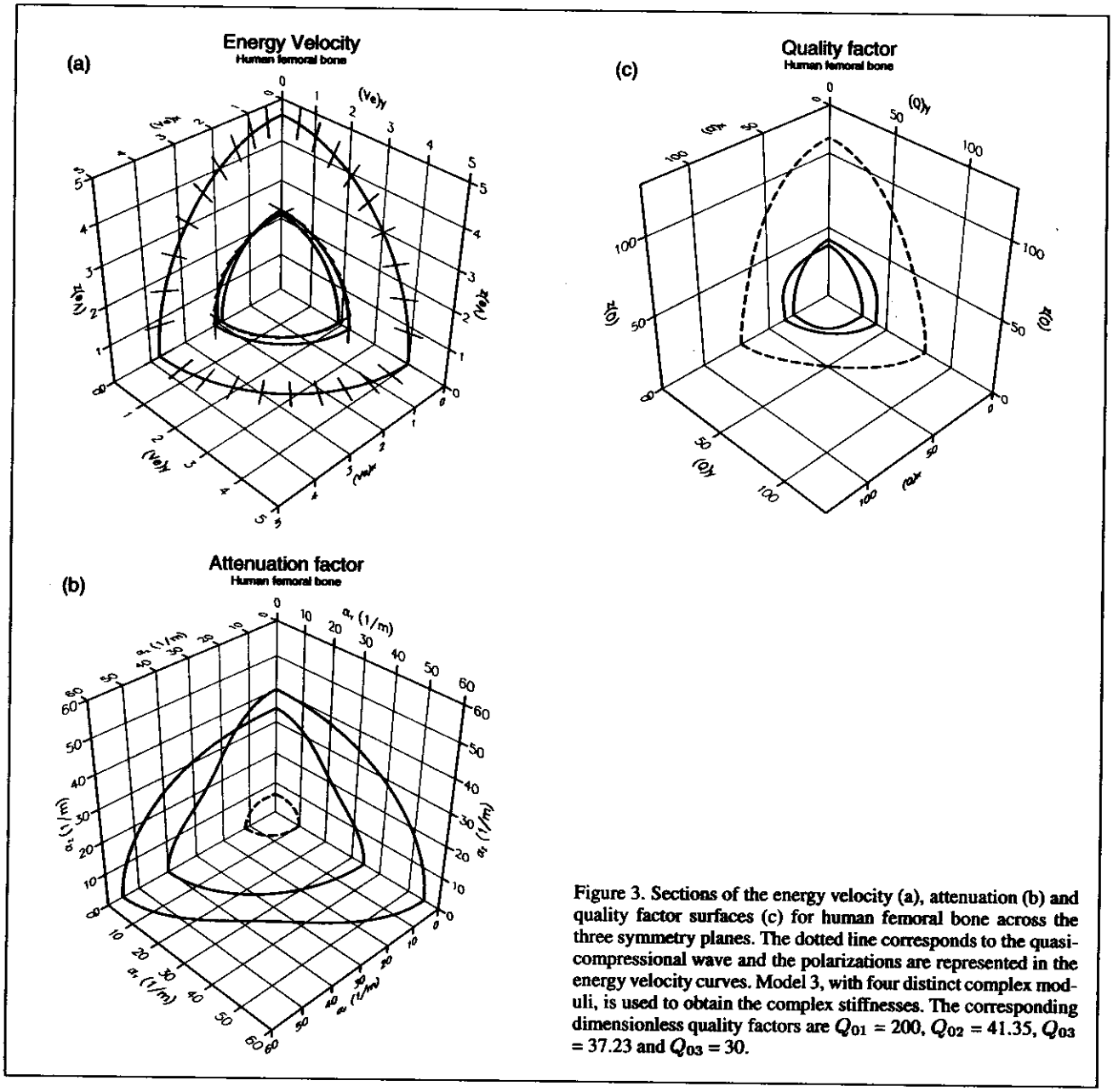


Figure 3. Sections of the energy velocity (a), attenuation (b) and quality factor surfaces (c) for human femoral bone across the three symmetry planes. The dotted line corresponds to the quasi-compressional wave and the polarizations are represented in the energy velocity curves. Model 3, with four distinct complex moduli, is used to obtain the complex stiffnesses. The corresponding dimensionless quality factors are $Q_{01} = 200$, $Q_{02} = 41.35$, $Q_{03} = 37.23$ and $Q_{03} = 30$.

sequence of two alternating layers, the explicit equations were obtained by Postma [16].

### 1.2. Model 2: Attenuation via eigenstrains

We introduce now a constitutive equation based on the fact that each eigenvector (called eigenstrain) of the stiffness tensor defines a fundamental deformation state of the medium. The six eigenvalues (called eigenstiffnesses) represent the genuine elastic parameters. For example, in the elastic case the strain energy is uniquely parameterized by the six eigenstiffnesses. From this fact and the correspondence principle we infer that in a real medium the rheological properties depend essentially on six relaxation functions, which are the generalization of the eigenstiffnesses to the viscoelastic case. The existence of six or less complex moduli depends on the symmetry class of the medium. The theory is developed in [7]. According to this approach, the principal steps in the construction of a viscoelastic rheology from a given stiffness tensor $C^{(e)}$ are the following:

1. Decompose the elastic stiffness tensor as

$$C^{(e)} = \sum_{I=1}^{6} \Lambda_I \, \mathbf{E}_I \otimes \mathbf{E}_I \, ,$$

where $\Lambda_I$ and $\mathbf{E}_I$ are the eigenvalues and normalized eigenvectors of $C^{(e)}$, respectively, and $\otimes$ denotes the tensor product. The elastic stability of the material ensures the symmetry of $C^{(e)}$; hence $\Lambda_I$ and $\mathbf{E}_I$ are real.

2. Invoking the correspondence principle, we get that a straightforward viscoelastic generalization of the above

equation – for time-harmonic motions of angular frequency $\omega$ – is given by

$$\mathcal{C}^{(v)} = \sum_{I=1}^{6} \Lambda_I \, M_I(\omega) \, \mathbf{E}_I \otimes \mathbf{E}_I \, ,$$

where $M_I(\omega)$ are complex moduli of the form 1. By construction, the eigenstiffnesses of $\mathcal{C}^{(v)}$ are complex, but the eigenstrains are the same as those of $\mathcal{C}^{(e)}$ and hence real.

For orthorhombic symmetry, the characteristic polynomial of the elasticity matrix, when in Kelvin's form, factors into the product of three linear factors and a cubic one: therefore, eigenstiffnesses are found by resorting to Cardano's formulae. For a transversely isotropic medium, the situation is even simpler, as the characteristic polynomial factors into the product of two squared linear factors and a quadratic one: a straightforward computation then yields that the independent entries of the complex stiffness matrix are, in Voigt notation,

$$p_{11} = \frac{\Lambda_4}{2} + \frac{\Lambda_1}{2+a^2} + \frac{\Lambda_2}{2+b^2}, \tag{7}$$

$$p_{12} = p_{11} - \Lambda_4, \tag{8}$$

$$p_{33} = \frac{a^2\Lambda_1}{2+a^2} + \frac{b^2\Lambda_2}{2+b^2}, \tag{9}$$

$$p_{13} = \frac{a\Lambda_1}{2+a^2} + \frac{b\Lambda_2}{2+b^2}, \tag{10}$$

$$p_{55} = \Lambda_3, \tag{11}$$

where

$$a = \frac{4c_{13}}{c_{11}+c_{12}-c_{33}-\sqrt{E}},$$

$$b = \frac{4c_{13}}{c_{11}+c_{12}-c_{33}+\sqrt{E}}, \tag{12}$$

and $\Lambda_I(\omega)$, $I = 1,\ldots,4$ are the complex and frequency-dependent eigenstiffnesses, given by

$$\Lambda_1 = \frac{1}{2}(c_{11}+c_{12}+c_{33}-\sqrt{E})M_1, \tag{13}$$

$$\Lambda_2 = \frac{1}{2}(c_{11}+c_{12}+c_{33}+\sqrt{E})M_2 \tag{14}$$

$$\Lambda_3 = 2c_{55}M_3, \tag{15}$$

$$\Lambda_4 = (c_{11}-c_{12})M_4, \tag{16}$$

with

$$E = 8c_{13}^2 + (c_{11}+c_{12}-c_{33})^2. \tag{17}$$

The two-fold eigenstiffnesses $\Lambda_3$ and $\Lambda_4$ are related to pure "isochoric" eigenstrains, i.e., to volume-preserving changes of shape only, while the single eigenstiffnesses $\Lambda_1$ and $\Lambda_2$ are related to eigenstrains that consist of simultaneous changes of volume and shape. For weak anisotropy, $\Lambda_1$ corresponds to the quasi-dilatational wave and $\Lambda_2$ to the quasi-shear wave. Moreover, $\Lambda_3$ and $\Lambda_4$ determine the $Q$ values of the shear waves along the principal axes.

### 1.3. Model 3: Attenuation via mean and deviatoric stresses

In this stress-strain relation [6, 8], the mean stress (i.e., the trace of the stress tensor) is only affected by the purely dilatational complex modulus $M_1$. Moreover, the deviatoric stress components solely depend on the shear complex moduli, denoted by $M_2$, $M_3$ and $M_4$. The trace of the stress tensor is invariant under transformations of the coordinate system. This fact assures that the mean stress depends only on $M_1$ in any system.

The complex stiffnesses for an orthorhombic medium are given by

$$p_{I(I)} = c_{I(I)} - D + KM_1 + \frac{4}{3}GM_\delta, \qquad I = 1,2,3, \tag{18}$$

$$p_{IJ} = c_{IJ} - D + KM_1 + 2G\left(1 - \frac{1}{3}M_\delta\right), \qquad I,J = 1,2,3;\ I \neq J, \tag{19}$$

$$p_{44} = c_{44}M_2, \quad p_{55} = c_{55}M_3, \quad p_{66} = c_{66}M_4, \tag{20}$$

where

$$K = D - \frac{4}{3}G \tag{21}$$

and

$$D = \frac{1}{3}\sum_{I=1}^{3} c_{II}, \quad G = \frac{1}{3}\sum_{I=4}^{6} c_{II}. \tag{22}$$

The index $\delta$ can be chosen 2, 3 or 4. Transverse isotropy implies equation (4), $M_4 = M_3 = M_2$ and $p_{66} = c_{66} + G(M_2 - 1)$.

This rheology has the advantage that the stiffnesses have a simple time domain analytical form, allowing the numerical solution of the viscoelastodynamic equations in the space-time domain.

## 2. Attenuation and quality factors

Substitution of the stress-strain relation for plane waves into the equations of momentum conservation gives the complex Christoffel equation. The eigenvalues of the Christoffel matrix are closely related to the complex velocities of the three propagating modes [8]. For homogeneous viscoelastic waves, the complex velocity $V$ is a fundamental quantity since it determines uniquely both the attenuation and the quality factors. For instance, the three waves propagating in the $(x,z)$-plane of an orthorhombic medium have the following velocities along the coordinate axes:

$$\begin{aligned} &V_{qS}(0) = V_{qS}(90) = \sqrt{p_{55}/\rho}, \\ &V_{qP}(0) = \sqrt{p_{33}/\rho}, \quad V_{qP}(90) = \sqrt{p_{11}/\rho}, \\ &V_{SH}(0) = \sqrt{p_{44}/\rho}, \quad V_{SH}(90) = \sqrt{p_{66}/\rho}, \end{aligned} \tag{23}$$

where 0 corresponds to the $z$-axis and 90 to $x$-axis. The magnitude of the attenuation vector is given by

$$\alpha = -\omega \mathrm{Im}(V^{-1}) \tag{24}$$

ACUSTICA · acta acustica
Vol. 84 (1998)

and the quality factor by

$$Q = \frac{\mathrm{Re}(V^2)}{\mathrm{Im}(V^2)} \tag{25}$$

[8]. Note that $V$ and $Q$ depend on the unrelaxed elasticities, the complex moduli and the propagation direction.

Attenuation and $Q$ factor are related by

$$\alpha = \omega \left( \sqrt{Q^2 + 1} - Q \right) \mathrm{Re}(V^{-1}). \tag{26}$$

For low-loss solids, where $Q \gg 1$, a Taylor expansion yields

$$\alpha \cong \frac{\omega}{2Q} \mathrm{Re}(V^{-1}) = \frac{\pi f}{Q V_{ph}}, \tag{27}$$

where $f$ is the frequency and $V_{ph}$ is the phase velocity given by

$$V_{ph} = [\mathrm{Re}(V^{-1})]^{-1}. \tag{28}$$

Equation (26) is the well-known relation between attenuation and quality factor [9].

In the case of inhomogeneous waves in weakly anisotropic TI media, the propagation and attenuation vectors are still expressible in closed forms, albeit more cumbersome [5]. In the next section both homogeneous and inhomogeneous waves will be used.

## 3. Examples

### 3.1. Hydrocarbon source rock

Shale source rocks have a very low porosity, and ultrasonic velocities normal to bedding are much lower than velocities parallel to bedding. In addition, they present a high level of wave attenuation [17], due to the kerogen content. Bakken shales, for instance [18], are a composite system made of illite, with velocities, densities and assumed $Q$ factors

$$V_P = 4.5 \text{ km/s}, \quad V_S = 3 \text{ km/s},$$

$$\rho = 2.7 \text{ g/cm}^3, \quad Q_1 = 80, \quad Q_2 = 60,$$

respectively; and kerogen, with velocities and $Q$ factors

$$V_P = 2.7 \text{ km/s}, \quad V_S = 1.5 \text{ km/s},$$

$$\rho = 1.4 \text{ g/cm}^3, \quad Q_1 = 30, \quad Q_2 = 20,$$

respectively. Let us assume that 60 percent of the shale is illite. Figure 1a shows a polar representation of the quality factor, corresponding to model 1. Only a quarter of the $(x, z)$-plane is plotted due to symmetry considerations. In the ideal case of parallel plane stratification, the quality factor curves obtained from model 1 approach the "exact" ones as the ratio of the thickness of the thickest layer to the pulse wavelength approaches zero [15]. Figures 1b and 1c display the curves for models 2 and 3, respectively, with parameters chosen so that their results be close to those of model 1, taken as giving synthetic data on which to test the flexibility of models 2 and 3. The best fit is obtained with model 2, since four kernels with $Q_{01} = 22$, $Q_{02} = 53$, $Q_{03} = 25.5$ and $Q_{04} = 62$ are used. Model 3 uses two kernels with $Q_{01} = 160$ and $Q_{02} = 22$, giving a quite good fit for the coupled modes and underestimating the value of the $S$-wave quality factor along the horizontal direction.

### 3.2. Orthorhombic media

The elasticity matrix representing the orthorhombic stiffness constants for human femoral bone is given in Voigt notation by [19]

$$\begin{pmatrix} 18 & 9.98 & 10.1 & 0 & 0 & 0 \\ 9.98 & 20.2 & 10.7 & 0 & 0 & 0 \\ 10.1 & 10.7 & 27.6 & 0 & 0 & 0 \\ 0 & 0 & 0 & 6.23 & 0 & 0 \\ 0 & 0 & 0 & 0 & 5.61 & 0 \\ 0 & 0 & 0 & 0 & 0 & 4.52 \end{pmatrix},$$

in GPa. Figure 2 shows sections of the energy velocity (a), attenuation (b) and quality factor surfaces (c) across the three symmetry planes, obtained with model 2. The dotted line corresponds to the quasi-compressional wave and the polarizations are represented in the energy velocity curves. The model uses six distinct complex moduli, whose dimensionless quality factors are defined as $Q_{0I} = [\Lambda_I(\infty)/\Lambda_6(\infty)]Q_{06}$, $I = 1, \ldots, 6$, with $Q_{06} = 30$.

The values of the quality factor along the symmetry axes for the inner curves are given by $Q_{0I}$, $I = 1, \ldots, 6$. We define the attenuation parameters for model 3 such that the $Q$ factors along the symmetry axes coincide with those of model 2, i.e, $Q_{01} = 200$, $Q_{02} = 41.35$, $Q_{03} = 37.23$ and $Q_{04} = 30$. Figure 3 shows sections of the energy velocity (a), attenuation (b) and quality factor surfaces (c) across the three symmetry planes, corresponding to model 3.

Although the $Q$ factors coincide along the cartesian axes (at least for the quasi-shear waves), the models yield quite dissimilar results out of the symmetry axes.

### 3.3. Modeling of experimental attenuation data

Yin [12] presents experimental results of stress-induced velocity and attenuation anisotropy of rocks. The following are the elastic constants of Massilon sandstone under triaxial loading conditions ($\sigma_{xx} = \sigma_{yy} = 1.72$ MPa, $\sigma_{zz} = 5.71$ MPa):

$$c_{11} = 16.97 \qquad c_{12} = 3.17$$
$$c_{13} = 4.39 \qquad c_{33} = 20.18$$
$$c_{55} = 7.75 \qquad c_{66} = 6.9$$

where the unit is GPa. For simplification of the analysis we assume that these elastic constants are unrelaxed, though the measurement is carried out at a finite frequency. On the other

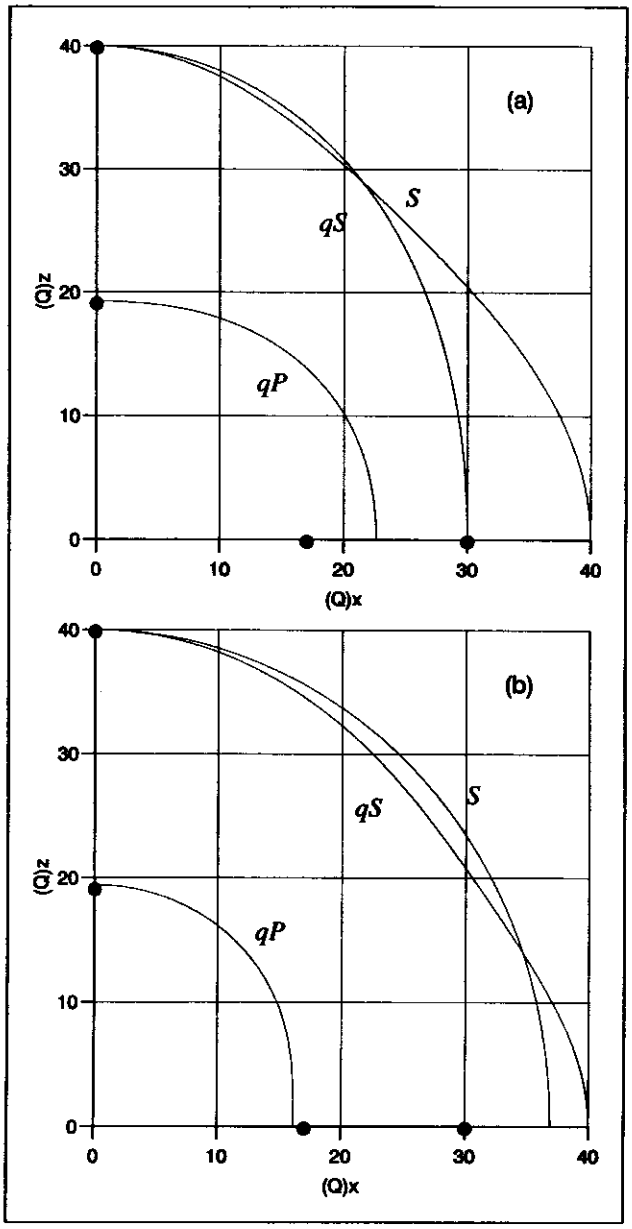


Figure 4. Polar representation of the quality factors for Massilon sandstone, corresponding to model 2 (a) and model 3 (b). The dots are the experimental values measured by Yin [12].

hand, Yin's quality factors versus the propagation angle $\theta$, measured from the axis of rotational symmetry, are

$$Q_{qP}(0) = 19.23$$
$$Q_{qP}(90) = 17.03$$
$$Q_{qS}(0) = 40.16$$
$$Q_{SH}(90) = 30$$

Figure 4 shows the quality factors corresponding to models 2 and 3. The experimental values are represented by dots. Model 2 uses three parameters to fit the data, with $Q_{02} = 15$, $Q_{03} = 40$, $Q_{04} = 30$ and $Q_{01} = Q_{03}$, while for model 3, $Q_{01} = 9.8$ and $Q_{02} = 40$. The latter describes fairly well the $qP$ factor.

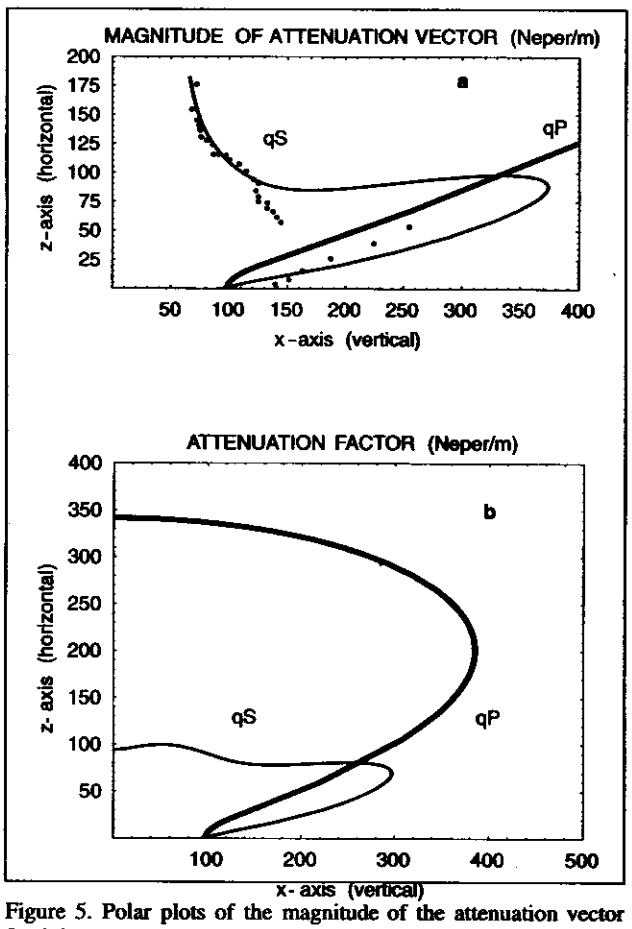


Figure 5. Polar plots of the magnitude of the attenuation vector for inhomogeneous waves (a) and attenuation coefficient (b) for homogeneous waves, corresponding to the quasi-longitudinal and quasi-shear waves. The data fitted refer to a transversely isotropic laboratory sample (Hosten *et al.*, [5]. The real part of the complex stiffnesses has been taken from [5], while its imaginary part has been computed from model 2 using $Q_{01} = 150$ (quasi-dilatational), $Q_{02} = 15$ (quasi-shear), $Q_{03} = 500$ (shear) and $Q_{04} = 5$ (shear).

Hosten *et al.* [5] obtained the following elastic constants for a carbon-epoxy composite:

$$c_{11} = 15 \qquad c_{12} = 7.7$$
$$c_{13} = 3.4 \qquad c_{33} = 87$$
$$c_{55} = 7.8 \qquad c_{66} = 3.9$$

given in GPa. They also obtained the imaginary part of the stiffness matrix by measuring the attenuation of inhomogeneous viscoelastic waves on a sample immersed in water. We recall that for inhomogeneous waves, equiphase planes do not coincide with equiamplitude planes. The best fit of the experimental data is obtained with model 2 (Figure 5a), with $Q_{01} = 150$, $Q_{02} = 15$, $Q_{03} = 500$ and $Q_{04} = 5$. Figure 5b shows the attenuation curves for homogeneous viscoelastic waves.

By comparing Figures 5a and 5b we conclude, as Hosten *et al.* [5], that homogeneous waves are inadequate to describe such anisotropic attenuation phenomena, whereas the analysis with inhomogeneous waves gives realistic results.

ACUSTICA · acta acustica
Vol. 84 (1998)

## 4. Conclusions

Because the anisotropic attenuation properties are closely related to the material symmetry given by the elastic constants, a proper anisotropic anelastic constitutive equation and a few experimental values of the quality factor should give a realistic description of the quality factor surfaces. This is confirmed by a test of two anelastic stress-strain relations on a composite material. However, application of the models to an orthorhombic medium yields quite dissimilar results out of the symmetry axes, where the $Q$ factor can be arbitrarily defined.

The emphasis in our paper is on constitutive laws, not on inversion algorithms. Thus, as a preliminary step towards a sound data-fitting procedure, we have used a naive trial-and-error procedure based on visual inspection. Therefore, our results may be viewed as encouraging rather than disappointing, although a quantitative error analysis is not yet possible and some slight misfit is still present, as in Figure 5a. In any case, the scarse available experimental data on anisotropic attenuation are not enough for a proper model verification.

## Acknowledgement

This work was supported in part by the Commission of the European Communities.

## References

[1] F. E. Neumann: Vorlesungen über die Theorie der Elastizität. Teubner, Leipzig, 1885.
[2] J. F. Nye: Physical properties of crystals - Their representation by tensors and matrices. Clarendon, New York, 1987.
[3] M. Fabrizio, A. Morro: Viscoelastic relaxation functions compatible with thermodynamics. J. Elasticity **19** (1988) 63–75.
[4] B. A. Auld: Acoustic fields and waves in solids. Robert E. Krieger, Publishing Co., Malabar, Florida, 1991.
[5] B. Hosten, M. Deschamps, B. R. Tittmann: Inhomogeneous wave generation and propagation in lossy anisotropic solids: Application to the characterization of viscoelastic composite materials. J. Acoust. Soc. Am. **82** (1987) 1763–1770.
[6] J. M. Carcione: Anisotropic $Q$ and velocity dispersion of finely layered media. Geophys. Prosp. **40** (1992) 761–783.
[7] J. M. Carcione, F. Cavallini: A rheological model for anelastic anisotropic media with applications to seismic wave propagation. Geophys. J. Int. **119** (1995) 338–348.
[8] J. M. Carcione, F. Cavallini: Attenuation and quality factor surfaces in anisotropic-viscoelastic media. Mech. of Mat. **19** (1995) 311–327.
[9] Seismic wave attenuation. Geophysical reprint series (1981).
[10] R. J. Arts, P. N. J. Rasolofosaon, B. E. Zinszner: Experimental determination of the complete anisotropic viscoelastic tensor in rocks. 62nd Ann. Internat. Mtg., Soc. Expl. Geophys., Expanded Abstracts, 1992. 636–639.
[11] S. Baste, B. Audoin: On internal variables in anisotropic damage. Eur. J. Mech. A / Solids **10** (1991) 587–606.
[12] H. Yin: Acoustic velocity and attenuation of rocks: isotropy, intrinsic anisotropy, and stress induced anisotropy. Dissertation. Stanford University, 1993.
[13] A. Ben-Menahem, S. G. Singh: Seismic waves and sources. Springer-Verlag, Berlin, 1981.
[14] M. M. Mehrabadi, S. C. Cowin: Eigentensors of linear anisotropic elastic materials. Q. J. Mech. appl. Math. **43** (1990) 15–41.
[15] G. E. Backus: Long-wave elastic anisotropy produced by horizontal layering. J. Geophys. Res. **67** (1962) 4427–4440.
[16] G. W. Postma: Wave propagation in a stratified medium. Geophysics **20** (1955) 780–806.
[17] D. H. Johnston: Physical properties of shale at temperature and pressure. Geophysics **52** (1987) 1391–1401.
[18] L. Vernik, A. Nur: Ultrasonic velocity and anisotropy of hydrocarbon source-rocks. Geophysics **57** (1992) 727–735.
[19] S. C. Cowin, M. M. Mehrabadi: On the identification of material symmetry for anisotropic elastic materials. Q. Jl. Mech. appl. Math. **40** (1987) 451–476.